Mathematical Models of the Geometry of Micro Milling Cutters

Alexander Isaev[1] , *Ramil* Khamzin[1], *Artem* Ershov[1] and *Marco* Leonesio[2]

[1]Moscow State University of Technology "STANKIN", RU-127055, Moscow, Russia
[2]Institute of Intelligent Industrial Technologies and Systems for Advanced Manufacturing of the National Research Council, STIIMA-CNR, IT-20133, Milano, Italy

Abstract. Micromachining is an up-to-date technology widely used in different advanced areas like electronics, aerospace and medical industries. For manufacturing components with highest precision and lowest surface roughness, small-sized end mills with working diameter of less than 1 mm are often used. In this paper, in order to determine the functional relationships between structural strength, cutting properties and geometry of small-sized cutting tools, the mathematical models of working part of micro milling cutters were derived.
Keywords. Micro milling cutter, micro machining, mathematical modelling.

1 Introduction

Micro cutting tools allows producing complex-shaped parts with high quality meeting the strict requirements for the components of electronics, aerospace, medical industry and others. The efficiency and effectiveness of micromachining depends on many variables including workpiece material properties, cutting tool parameters [1-8], process parameters, machine tool characteristics and many others.

When micro cutting the advanced materials such as titanium and its alloys, it is of highly important to take into account their physical and mechanical properties causing certain difficulties in their machining such as relatively low modulus of elasticity produces vibrations during cutting, low ductility causes negative chip shrinkage, low thermal conductivity and high heat resistance intensively generate heat which affects the heat balance during machining with heat transfer through cutting tool resulting in increased tool wear, relatively low modulus of elasticity producing vibrations and chattering during cutting, and chemical interactions with gases at elevated temperatures appearing during cutting that increase the hardness of workpiece superficial layer [2,3,4,7]. To increase tool life, the cutting geometry of micro milling cutters should be thoroughly analysed at the design stage. For dynamically unstable milling process, the actual values of kinematic clearance angles depending on the process parameters should be calculated.

2 Methods

2.1 Influence of rounding radius of the cutting edge on cutting data parameters

The efficiency of chip formation during milling is largely determined by the ratios f_z/ρ and a_e/ρ, where f_z is the feed per tooth, a_e is the width of cut, ρ is the cutting edge rounding radius (Fig.1). These conditions are especially important when machining with small-sized milling cutters. When feed per tooth and cutting depth are lower than the rounding radius, i. e. $f_z < \rho$ and $a_e < \rho$, the cutting capacity of the milling tooth get worse. In this case, the actual rake angle becomes negative, consequently instead of cutting the intensive wear of workpiece material is observed leading to the increase of cutting forces. The compression deformations in the contact layer of the workpiece material produce wear hardening [5]. This worsens the cutting conditions for the following cutting tooth. The same effects present in up-milling where at the tooth entrance the thickness of the cut layer is zero.

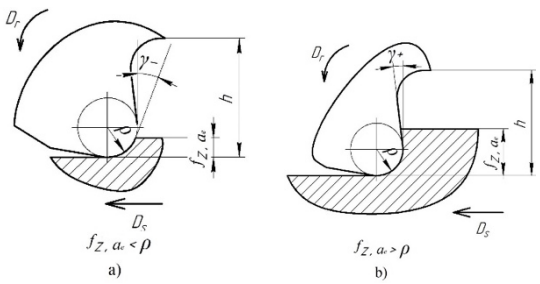

Fig. 1. Cutting edge rounding radius related to the cutting data parameters: a) conditions for inefficient chip formation, b) conditions for effective chip formation

During manufacturing of the cutting tool, the value of ρ is affected by the parameters as follows [9-22]:

- cutting material grade and its grain and pore size;
- wear resistant coating deposition parameters, process parameters, i. e. grinding wheel parameters, grinding speed, feed rate and cutting depth;
- roughness of rake and flank surfaces;
- wear resistant coating deposition parameters;
- process parameters, i. e. grinding wheel parameters, grinding speed, feed rate and cutting depth;

To determine the minimum allowable values of the process parameters required for stable chip formation, the geometry of a micro milling cutter of the GF500T series manufactured by Guhring was analyzed. According to the manufacturer's catalog, the end mill has the following geometric parameters: outer diameter d=0.5 mm, helical angle $\omega=30^{o}$, peripheral rake angle $\gamma=8^{o}$, and the corner radius R=0.01 mm. The recommended cutting data for processing titanium alloys are: feed per tooth f_z = 0.007 mm/tooth, width of cut a_e=0.1 mm, axial depth of cut a_p=0.05 mm.

The general geometrical parameters of the micro end mill were measured using measuring machine Walter Helicheck Plus. The cutting edge rounding radii were measured with GFM MikroCAD premium+ Microscope. It was found that the rake angle measured at a distance of 0.6 mm from the tool top is negative and is equal to 2pprox.. -8^{o}. The cutting edge rounding radius is irregular and takes values in the range of 7…9 μm in different cross-sections normal to the helical cutting edge (Table 1).

2.2 Mathematic models for calculating a cutting speed angles and working kinematic clearance angles for down and up milling

During the cutting, both the angle of cutting speed η and the working kinematic clearance angle α_p measured between the flank surface and the direction of the resultant cutting speed change. The behavior of the angle η is affected by the milling direction. When down milling, at the point of engagement into the material, the angle η has the maximum value and gradually decreases with moving to the point of disengagement, increasing the value of the angle α_p. In up-milling, the angle η gradually increases as the cutter engages into the material thereby reducing the working clearance angle α_p (Fig. 2).

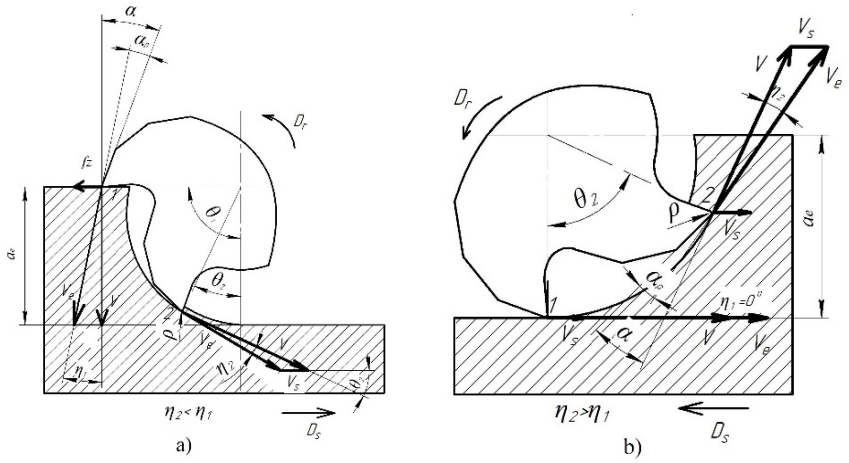

Fig. 2. Change of the angle η n the working plane at different moments of the working stroke of the mill: a – in down-milling, $\eta_2 < \eta_1$, b – in up-milling, $\eta_2 > \eta_1$; 1 – the point at the moment when the cutting edge engages into the workpiece, 2 – the point engaged into the workpiece; V – the velocity of the main cutting movement at the considered cutting point; V_e – the velocity of the resulting cutting speed; V_s – the velocity of the feed; η – the cutting speed angle; θ_1, θ_2 – the angles of contact of cutting tooth with the workpiece surface at the engagement and at some instance, respectively; a_e – the radial depth of cut; α_p – the kinematic clearance angle in the working plane; α – the clearance angle, ρ – the cutting edge rounding radius

With the decrease in the angle α_p, a greater amount of heat is absorbed by cutter thus reducing the tool life and deteriorating the surface quality due to decreasing clearance between the flank and the workpiece surfaces, especially when machining using micro end mills.

To create mathematical models for calculating the α_p angle basing on the cutting data, the schemes of milling process in the working plane (Fig. 3) are used. The kinematic clearance angle is equal to:

$$\alpha_p = \alpha - \eta \qquad (1)$$

Table 1. Designed geometry (from catalogue) compared with actual geometrical parameters of micro milling cutters

	Outer diameter *d*, mm	**Helical angle ω, °**	**Peripheral rake angle γ, °**	**Corner radius R, mm**	**Cutting edge rounding radius ρ, mm**
Catalog data	0,5	30	8,0	0,01	N/A
Measured data (ID 1)	0,486	30,05	-8,4	0,01	7…9
Measured data (ID 2)	0,478	28,4	4,03	0,01	7…8

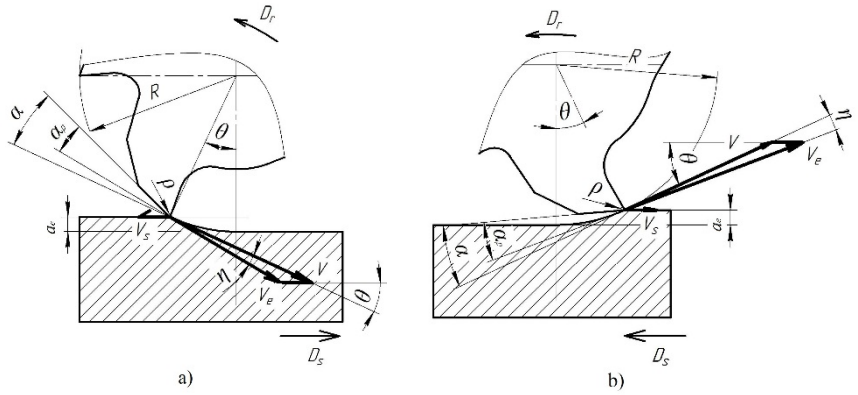

Fig. 3. Schemes of milling for determination the angles η and α_p, a – in down milling, b – in up-milling, V – the velocity of the main cutting movement at the considered cutting point; V_e – the velocity of the resulting cutting speed; V_s – the velocity of the feed; η – the cutting speed angle; θ_1, θ_2 – the angles of contact of cutting tooth with the workpiece surface at the engagement and at some instance, respectively; a_e – the radial depth of cut; α_p – the kinematic clearance angle in the working plane; α – the clearance angle, ρ – the cutting edge rounding radius, D_s – the feed velocity, D_r – the main cutting movement velocity

To determine the speed of the resulting velocity $\mathbf{V_e}$ we should first calculate the contact angle θ:

$$\cos\theta = 1 - \frac{t}{R} \tag{2}$$

According to the diagram in Fig. 3, we can express the resulting cutting speed
- for down-milling:

$$\boldsymbol{V_e^2} = \mathbf{V}^2 + \mathbf{V_s}^2 - \mathbf{2}\boldsymbol{V}\boldsymbol{V_s}\cos\theta \tag{3}$$

- for up-milling:

$$\mathbf{V_e^2} = \mathbf{V^2} + \mathbf{V_s}^2 - 2\mathbf{V}\mathbf{V_s}\,cos(180 - \theta) \tag{4}$$

- for up- and down-milling:

$$\mathbf{V_s}^2 = \mathbf{V}^2 + \mathbf{V}_e^2 - 2\mathbf{V}\mathbf{V_e}\cos\eta \tag{5}$$

Taking into account (1), the equations (2–4) take the form:

$$V_e^2 = (2\pi R)^2 + {f_z}^2 - 4\pi R S_z(1 - \frac{a_e}{R}) \tag{6}$$

$$V_e^2 = (2\pi R)^2 + {f_z}^2 - 4\pi R S_z(\frac{a_e}{R} - 1) \tag{7}$$

$${f_z}^2 = (2\pi R)^2 + V_e^2 - 4\pi R V_e\cos\eta \tag{8}$$

From equation (7) we obtain:

$$\cos\eta = \frac{(2\pi R)^2 + \mathbf{V_e^2} - {f_z}^2}{4\pi R\mathbf{V_e}} \tag{9}$$

Substituting equations (6) and (7) into equation (9) and simplifying it, we obtain the mathematical models for calculating:
- the angle of the cutting speed during down-milling:

$$\eta = \arccos(\frac{2\pi R^2 - f_z R + f_z a_e}{R\sqrt{(2\pi R - f_z)^2 + 4\pi f_z a_e}}) \tag{10}$$

- the angle of the cutting speed during up-milling:

$$\eta = \arccos(\frac{2\pi R^2 - f_z a_e + f_z R}{R\sqrt{(2\pi R + f_z)^2 - 4\pi f_z a_e}}) \tag{11}$$

Finally, we obtain the mathematical models for calculating the α_p angle
- for down-milling:

$$\alpha_p = \alpha - \arccos(\frac{2\pi R^2 - f_z R + f_z a_e}{R\sqrt{(2\pi R - S_z)^2 + 4\pi f_z a_e}}) \tag{12}$$

- for up-milling:

$$\alpha_p = \alpha - \arccos(\frac{2\pi R^2 - f_z a_e + f_z R}{R\sqrt{(2\pi R + f_z)^2 - 4\pi f_z a_e}}) \tag{13}$$

The obtained mathematical models allow us to determine in the working plane the dependence of the α_p

angle on the milling width a_e and the feed f_z for end mills of different diameters. The mathematical models determine the maximum value of the α_p angle: for down-milling at the engagement of the milling tooth into the workpiece, and for up-milling at the disengagement of the milling tooth from the workpiece.

For micro milling cutters with helical teeth, the geometric parameters in the working plane relate to the geometric parameters in the normal cutting plane as follows:

$$\tan \alpha_n = \frac{\tan \alpha_p}{cos\omega}, \quad (14)$$

where α_n is the clearance angle in the normal secant plane to the main cutting edge, α_p is the clearance angle in the working plane, ω is the helix angle. Therefore, $\alpha_n < \alpha_p$.

2.3 Analysis of kinematic clearance angles of micro end mill

The obtained mathematical models allow determining the dependence of the working kinematic clearance angle α_p on 3 variables, i. e. the working radius of the micro end mill, the radial depth of cut a_e and the feed per tooth f_z measured in different cutting directions. To determine what parameter is the most influential on changing the kinematic clearance angle, it is necessary to define their influence separately. To do this, the dependency graphs of the kinematic clearance angle for micro end mills with the diameters d=1 mm and d=0.5 mm and clearance angle 17° were plotted according to the obtained mathematic models with the following parameters:

- radial depth of cut a_e with the feed per tooth f_z=0,02d (Fig. 4a) and f_z= 0.01, 0.03 and 0.05 mm/tooth (Fig. 5);
- feed per tooth f_z with the radial depth of cut a_e=0,05d (Fig. 5b) and a_e= 0,01, 0,03, 0,05 mm (Fig. 6).

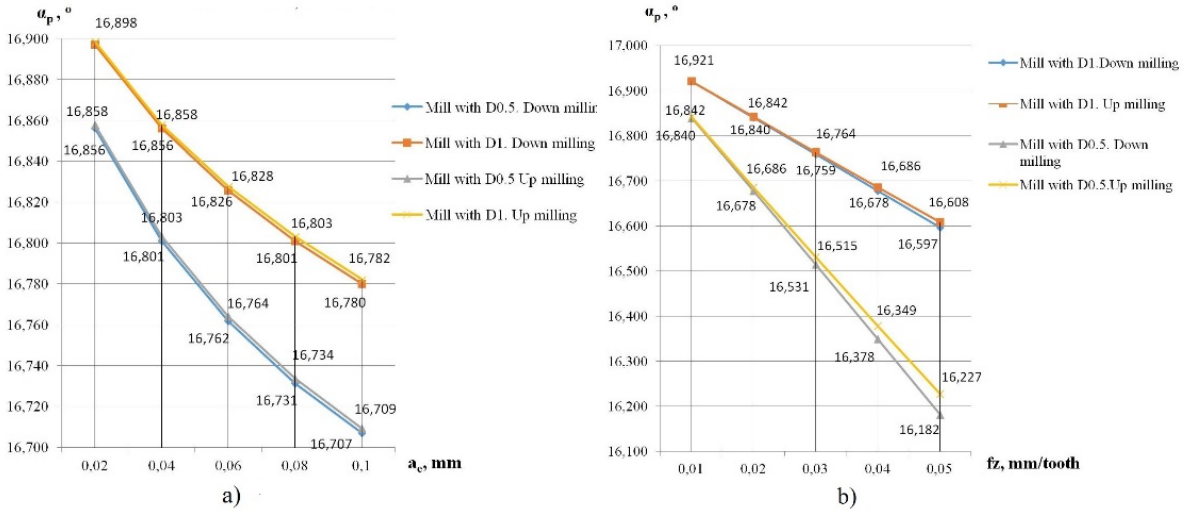

Fig. 4. Dependencies of the kinematic clearance angle α_p for micro end mills with d=1mm and d=0.5mm both having clearance angle α=17° on: a) radial depth of cut a_e with feed per tooth f_z=0.05d; b) feed per tooth f_z with radial depth of cut a_e=0.05d

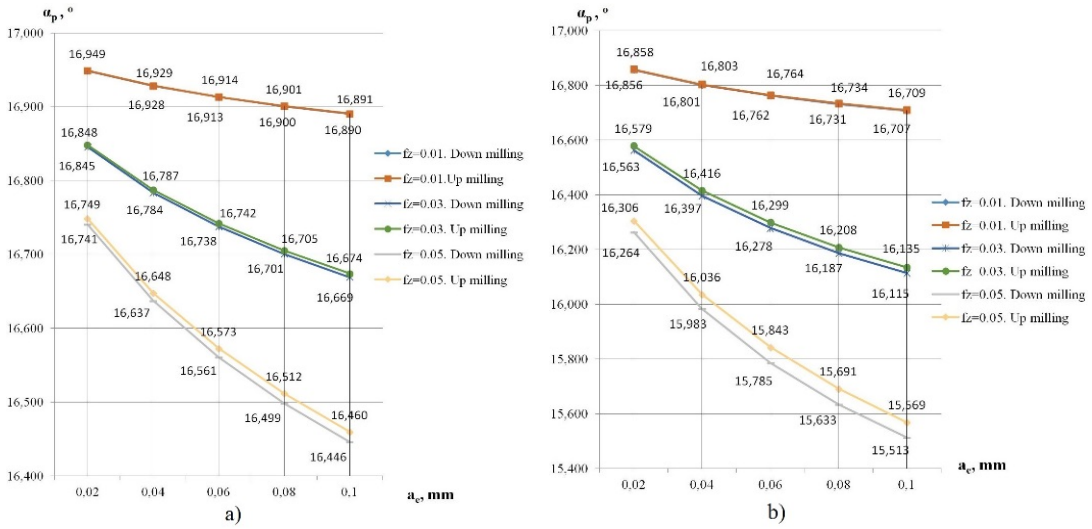

Fig. 5. Dependencies of the kinematic clearance angle α_p on radial depth of cut a_e with feeds per tooth of 0.01, 0.03 and 0.05 mm for micro end mills: a) d=1 mm, b) d=0,5m

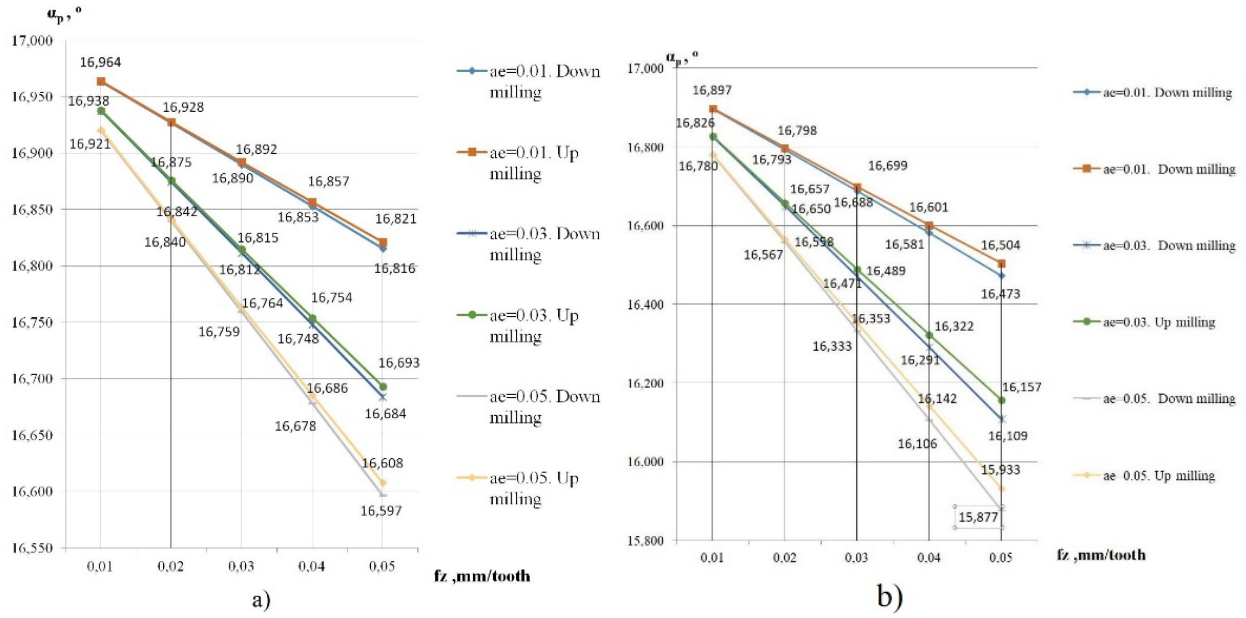

Fig. 6. Dependencies of the kinematic clearance angle on feed per tooth f_z with radial depth of cut a_e=0.01, 0.03 and 0.05 mm for micro end mills: a) *d*=1 mm, b) *d*=0,5mm

According to the graph of dependence $\alpha_p(f_z)$ shown in Fig. 4b and 6, a hypothesis for a linear dependence between these parameters was introduced. To confirm this hypothesis and to define a shape of the function $\alpha_p(f_z)$, we have used the approximation tools of the Microsoft Excel. Using this software, the linear function was defined as the most accurate approximation of dependence between the kinematic clearance angle and the feed per tooth since its coefficient of determination has the maximum possible value, R^2=1. The most relevant approximation type for the dependence of kinematic clearance angle α_p on the radial with of cut a_e is a polynomial function of second order. Therefore, the relationship between α_p and f_z has the following form:

$$\alpha_p(f_z) = -Af_z + B \quad (15)$$

The functional relationship between α_p and a_e is as follows:

$$\alpha_p(a_e) = Aa_e^2 - Ba_e + C, \quad (16)$$

where *A*, *B* and *C* are the function coefficients.

Using the cutting conditions recommended for machining the titanium alloys with micro end mills GF500T by Guhring, the graph plots (Fig. 7) were constructed. The graph plot for the $\alpha_p(a_e)$ at such cutting conditions is approximated by the linear function. Basing on this statement, the calculation of coefficients was performed and the separate influence of parameters a_e and f_z on the value of the angle α_p was identified.

To calculate the coefficients *A* and *B* in (15) and (16), the least squares method was used as follows:

$$A = \frac{n\sum f_{zi}\alpha_{p_i} - \sum f_{zi}\sum \alpha_{p_i}}{n\sum f_{zi}^2 - \sum f_{zi}\sum f_{zi}} \quad (17)$$

$$B = \frac{\sum \alpha_{p_i}\sum f_{zi}^2 - \sum f_{zi}\sum f_{zi}\alpha_{p_i}}{n\sum f_{zi}^2 - \sum f_{zi}\sum f_{zi}}, \quad (18)$$

where f_{zi} is the *i*-th value of feed per tooth; α_{pi} is the i-th value of kinematic clearance angle with *i*-th value of feed per tooth; *n* is the total number of values.

Taking into account the calculated values of *A* and *B*, the equation for the kinematic clearance angle depending on the feed per tooth for up-milling (line 2 in Fig. 7) takes the following form:

$$\alpha_p(f_z) = -21{,}230f_z + 18{,}054 \quad (19)$$

For down milling (Fig. 7, line 1):

$$\alpha_p(f_z) = -22{,}568f_z + 18{,}136 \quad (20)$$

The values of *A* and *B* in (17) and (18) are also calculated using the same method of least squares:

$$A = \frac{n\sum a_{ei}\alpha_{p_i} - \sum a_{ei}\sum \alpha_{p_i}}{n\sum a_{ei}^2 - \sum a_{ei}\sum a_e} \quad (21)$$

$$B = \frac{\sum \alpha_{p_i}\sum a_{ei}^2 - \sum a_{ei}\sum a_{ei}\alpha_{p_i}}{n\sum a_{ei}^2 - \sum a_{ei}\sum a_{ei}}, \quad (22)$$

where a_{ei} is the *i*-th value of the radial depth of cut; α_{pi} is the *i*-th value of a kinematic clearance angle at *i*-th value of radial depth of cut; *n* is the total number of reference values. Thus, the equation of the kinematic clearance angle depending on the radial depth of cut for up-milling (Fig. 7, line 4) is as follows:

$$\alpha_p(a_e) = -0{,}956a_e + 16{,}891 \quad (23)$$

For down milling (Fig. 7, graph 3) the equation of dependence looks:

$$\alpha_p(a_e) = -0{,}956a_e + 16{,}890 \qquad (24)$$

In the derived pairs of equations (19), (20) and (23), (24), the difference between coefficients A is more pronounced than the difference between coefficients B. Moreover, the value of A in equations (23) and (24) is greater than one in formulas (19) and (20). Thus, the feed per tooth at the recommended cutting conditions is more influential on the kinematic clearance angle α_p than the radial depth of cut.

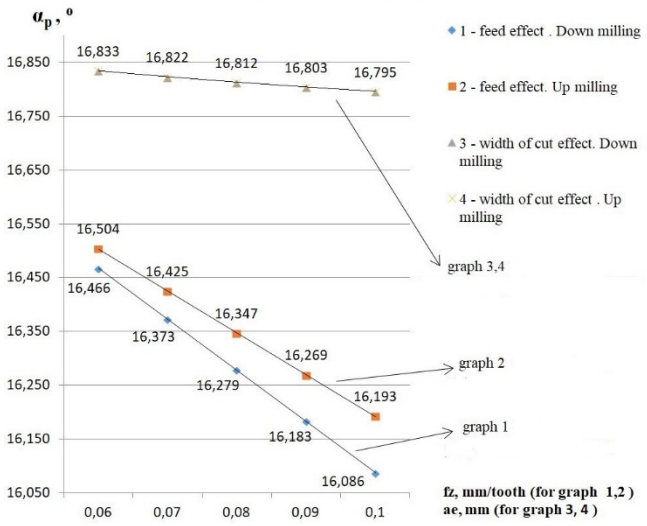

Fig. 7. Graph plots and equations of the kinematic clearance angle α_p depending on depth per tooth and radial width of cut with the recommended cutting data a_e=0,1 mm and f_z=0,007 mm/tooth for micro end mills with GF500T by Guhring with d=0.5mm

3 Results and discussion

The created mathematical models allow designing micro end mills with the geometrical parameters optimal in strength and determining the range of optimal feed values and width of cut a_e which must meet the conditions $\rho < f_z < h$ and $\rho < a_e < h$.

According to the measurement protocol, the cutting edge radius is irregular along the helical cutting edge having the values in the range of 7…9 μm. For small-sized milling cutters, the cutting edge radius variation of 25% is very significant since at the recommended feed per tooth f_z = 0.007 mm the chip formation is inefficient in all cross-sections.

The actual measured value of the rake angle on the peripheral part of helical cutting edge turned out to be negative instead of the positive value showed in the catalog. This may result in significant variability in cutting process parameters when milling. At the same time, the negative geometry is a feasible solution for micro milling cutters made of advanced materials like reinforced cutting ceramics. These kinds of cutting tools may be suitable for use in machining medical components made of nickel and cobalt alloys because the negative design makes the cutting edge stiffer and stronger.

4 Conclusions

The derived mathematical models allow designing micro end mills with the geometry optimal in strength. These mathematical models can be used to determine the reasonable range of optimal cutting data for micro milling process.

The negative values of rake angle acquired from measuring machine do not correspond with the catalog of the micro milling cutter manufacturer. Alternatively, the negative cutting geometry can be used for micro end mills made of cutting ceramics because this design feature makes the cutting edge stiffer and stronger.

With decreasing diameter of micro end mill, the influence of feed per tooth f_z and a_e on the kinematic clearance angle α_p increases.

The difference between the values of the kinematic clearance angle α_p for the down and up milling increases with growing a_e and f_z and with decreasing diameter of the micro end milling cutter.

The feed per tooth f_z has a greater effect on the change of the kinematic clearance angle α_p than the radial depth of cut a_e. The dependence function of $\alpha_p(a_e)$ has a polynomial form, and, in this case, second-order polynomial is the most suitable approximation.

Acknowledgments

This research was funded by Ministry of Science and Higher Education of the Russian Federation, Grant No. 0707-2020-0031. This work was carried out using equipment provided by the Center of Collective Use of MSUT "STANKIN".

References

1. V.V. Kuzin, S.N. Grigoriev, M.Yu. Fedorov, Part 2: Microlevel, J. Frict. Wear, **36**(1), 40-44 (2015)
2. M.A. Volosova, S.N. Grigor'ev, V.V Kuzin, Part 4. Action of Heat Flow. Refract Ind Ceram, **56**, 91–96 (2015)
3. A.A. Vereschaka, S.N. Grigoriev, N.N. Sitnikov, A. Batako, Surface and Coatings Technology, **332**, 198-213 (2017)
4. V.V. Kuzin, S.N. Grigor'ev, M.A. Volosova, Refract. Ind. Ceram., **54**, 376–380 (2014)
5. S.N. Grigoriev, O.V. Sobol, V.M. Beresnev, I.V. Serdyuk, A.D. Pogrebnyak, D.A. Kolesnikov, U.S. Nemchenko, J. Frict. Wear, **35**(5) 359-364 (2014)
6. A.S. Metel, S.N. Grigoriev, Yu.A. Melnik, V.P. Bolbukov, Instrum. Exp. Tech., **55**(1), 122-130 (2012)
7. A. Metel, V. Bolbukov, M. Volosova, S. Grigoriev, Yu. Melnik, Instruments and Experimental Techniques, **57**(3), 345–351 (2014)
8. O.V. Sobol', A.A. Andreev, S.N. Grigoriev, V.A. Stolbovoy, Problems of Atomic Science and Technology, **4**, 174-177 (2011)

9. A. Metel, V. Bolbukov, M. Volosova, S. Grigoriev, Y. Melnik, Surf. Coat. Technol., **225**, 34-39 (2013)
10. D.S. Rechenko, A.G. Kol'tsov, Russ. Eng. Res., **32**(2), 179-181 (2012)
11. S. Grigoriev, Y. Melnik, A. Metel, Surf. Coat. Technol. **156**(1–3), 44–49 (2002)
12. V. Grechishnikov, S. Grigoriev, P. Pivkin, M. Volosova, A. Isaev, D. Nikitin, I. Minin, EPJ Web of Conferences, **224**, 05001 (2019)
13. X. Kong, Z. Ding, L. Xu, L. Zhu, J. Zhang, C. Wu, A. Isaev, EPJ Web of Conferences, **224**, 05009 (2019)
14. V.A. Grechishnikov, Y.E. Petukhov, P.M. Pivkin, et al. Meas Tech., **58**, 848–853 (2015) https://doi.org/10.1007/s11018-015-0806-z
15. I.A. Kovalev, P.A. Nikishechkin, A.S. Grigoriev. 2017 International Conference on Industrial Engineering, Applications and Manufacturing (ICIEAM), St. Petersburg, 1-4 (2017)
16. S.N. Grigoriev, P.M. Pivkin, V.A. Grechishnikov, Y.E. Petukhov, M.A. Volosova, A.B. Nadykto, Proc. SPIE (International Society for Optics and Photonic, **11540**, 115401E, 2020)
17. S.N. Grigoriev, M.A. Volosova, A.A. Okunkova, S.V. Fedorov, K. Hamdy, P.A. Podrabinnik, ... , A.N. Porvatov, J. Manuf. Mater. Process., **4**(3), 96 (2020) https://doi.org/10.3390/jmmp4030096
18. P.M. Pivkin, A.B. Nadykto, V.A. Grechishnikov, M.A. Volosova, I.V. Minin, S.N. Grigoriev, Proc. SPIE (International Society for Optics and Photonic, **11540**, 115401G, 2020)
19. I.A. Kovalev, M.S. Babin, P.A. Nikishechkin., MATEC Web of Conferences, **298**, 00110. (2019)
20. S. Grigoriev, M. Volosova, V. Grechishniko, P. Pivkin, P. Peretyagin, A. Zelensky, Proc CIRP, **95**, 337-342 (2020)
21. D.S. Rechenko, A.V. Popov, K.V. Averkov, V.A. Sergeev, Russ. Eng. Res., **32**(5-6), 511-512 (2012)
22. P.A. Nikishechkin, N.S. Grigoriev, N.Yu. Chervonnova, MATEC Web of Conferences, **298**, 00064 (2019)